

Subthreshold Antiproton Production in $^{28}\text{Si} + ^{28}\text{Si}$ Collisions at 2.1 GeV/Nucleon

J. B. Carroll,⁽¹⁾ S. Carlson,⁽¹⁾ J. Gordon,⁽¹⁾ T. Hallman,⁽⁴⁾ G. Igo,⁽¹⁾ P. Kirk,⁽⁵⁾ G. F. Krebs,⁽³⁾ P. Lindstrom,⁽³⁾ M. A. McMahan,⁽³⁾ V. Perez-Mendez,⁽³⁾ A. Shor,⁽²⁾ S. Trentalange,⁽¹⁾ and Z. F. Wang⁽¹⁾

⁽¹⁾University of California at Los Angeles, Los Angeles, California 90024

⁽²⁾Brookhaven National Laboratory, Upton, New York, 11973

⁽³⁾Lawrence Berkeley Laboratory, Berkeley, California 94720

⁽⁴⁾Johns Hopkins University, Baltimore, Maryland 21218

⁽⁵⁾Louisiana State University, Baton Rouge, Louisiana 70803

(Received 12 December 1988; revised manuscript received 16 February 1989)

We report on the first observation of subthreshold antiproton production in nucleus-nucleus collisions. This measurement was made for the system $^{28}\text{Si} + ^{28}\text{Si}$ at a bombarding energy of 2.1 GeV/nucleon (kinetic energy per NN pair in the c.m. frame ~ 850 MeV). A differential cross section $d^2\sigma/dP d\Omega$ of 80 ± 40 nb/sr (GeV/ c) was measured for \bar{p} production at 1.9 GeV/ c and 0° . This result is 3 orders of magnitude larger than that predicted by a calculation incorporating internal motion of the nucleons in the colliding nuclei.

PACS numbers: 25.70.Np

Subthreshold production of particles in nucleus-nucleus collisions may probe collective effects that are not easily accessible through other techniques. Subthreshold pion production has been studied in a number of experiments¹⁻⁴ but is limited to low excitation energies and, except for collisions between very massive systems,⁴ the production process is strongly influenced by the effects of interactions in either the initial state ("Fermi momentum"), the final state (production of bound nuclei), or both. The production of more massive particles permits the study of collectivity at higher excitation energies and in regions of final-state phase space where the above influences do not apply. The results of a recent survey of subthreshold K^- production⁵ may contain indications of collective behavior, but since some of this yield can arise from strangeness exchange in intermediate states ($Y + \pi \rightarrow N + K^-$), a firm conclusion awaits more detailed analysis. Subthreshold production of antiprotons has no equivalent quantum-number exchange and, as will be discussed later, internal nuclear momentum of the incident projectile and target nucleons cannot account for antiproton production at the levels reported here.

We report here on the first observation of subthreshold antiproton production in nuclear collisions. The experiment was performed at the Lawrence Berkeley Laboratory Bevalac in a beam line which was specifically designed for subthreshold K^- and \bar{p} measurements. The spectrometer consisted of a secondary beam line with two magnetic bends, two sets of focusing elements, and detector stations at the two beam foci. A 25° bend beginning immediately downstream from the target separated the negative secondaries from the positively charged nuclear debris. A brass collimator at the first focus defined the secondary momentum acceptance to be $\Delta P/P \sim 1.5\%$. This collimator was built into a massive

shielding enclosure that isolated the detector stations from the areas containing the target and primary beam. The first detector station contained two fast scintillation counters for time-of-flight (TOF) measurements,—one directly downstream of the collimator and the second 2 m further downstream—a focusing liquid Cherenkov counter ($\beta_{\text{thres}} \sim 0.9c$), and two aerogel Cherenkov counters ($\beta_{\text{thres}} \sim 0.98c$). The second detector station contained a third fast TOF scintillation counter, a focusing liquid Cherenkov counter, one aerogel counter, several beam-defining counters, and a lead-glass array at the end of the line for measuring total deposited energy. The total length of the lead-glass array was about 2 interaction lengths. A charge-coupled-device (CCD) electronic readout of the first and third TOF counters sampled the pulse heights at 5-ns intervals to identify pileup events. The total acceptance of the line was $\Delta\Omega \sim 5$ msr. The distance between the first and third TOF counter was 7.5 m (25 ns). A detailed description of the apparatus will be given elsewhere.⁶

The measurements reported here are for the reaction $^{28}\text{Si} + ^{28}\text{Si}$ at 2.1 GeV/nucleon (kinetic energy per NN pair in the c.m. frame is 855 MeV). The secondary line was tuned for 1.89-GeV/ c negative particles produced at 0° . The beam intensity (measured with a calibrated ion chamber) was $\sim 10^9$ /spill, and the production target was 16 g/cm² thick, which is approximately one-half of an interaction length for Si+Si. The total run lasted 21 h. The main trigger consisted of a coincidence between several of the scintillation counters and a veto from at least two of the aerogel counters. A prescaled trigger containing no veto provided a large data sample for calibration and diagnostics. Time and pulse-height information from all photomultipliers were digitized and recorded for each event. The off-line analysis contained cuts to define clean events with no pileup, and various Cheren-

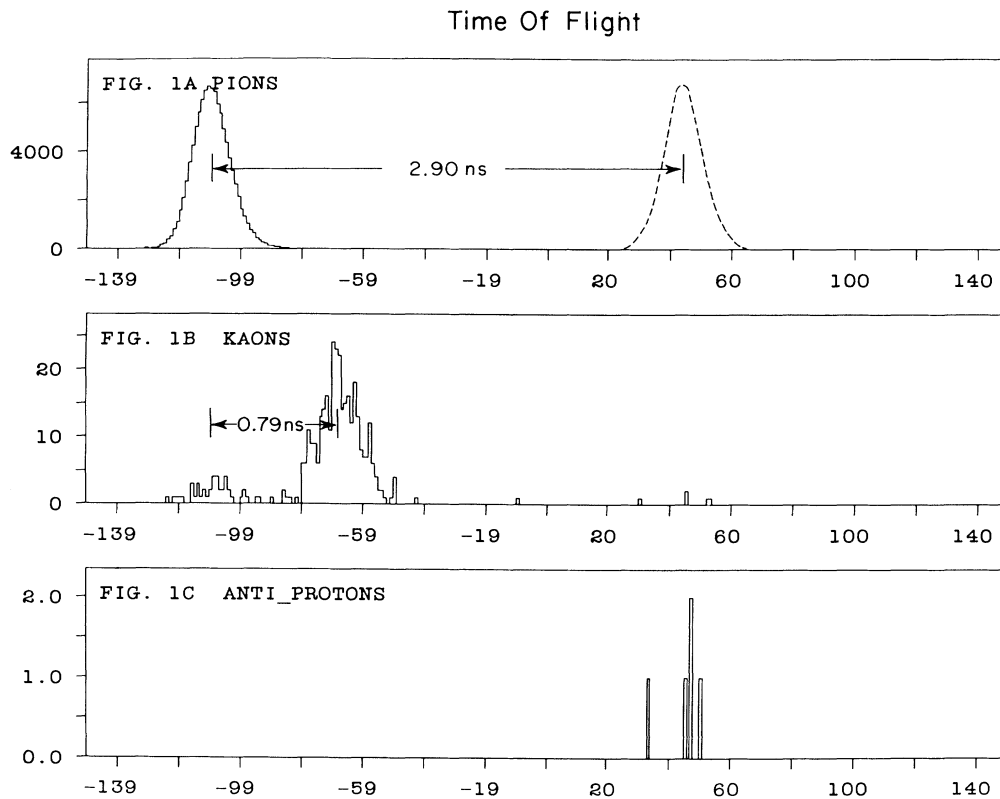


FIG. 1. TOF distribution between the first and second detection areas (~ 25 ft). TOF for (a) events which trigger aerogel Cherenkov counters, (b) events with no aerogel signal, and (c) events with no aerogel or liquid Cherenkov signal.

kov cuts to identify the pion and kaon background. The TOF was corrected for shifts by monitoring the positions of the pion and kaon peaks.

Figure 1 shows spectra of the time of flight between the first TOF counter in detector station 1, and the TOF counter in detector station 2. Figure 1(a) is the TOF spectrum for events with a signal in all Cherenkov counters. The peak is identified as pions and has a σ of 110 ps. Figure 1(b) is the TOF for events with no signal in the aerogel counters. A clear K^- peak is seen. Figure 1(c) shows events with no signal in either the aerogel or liquid Cherenkov counters. Of the 1.94×10^7 pion pretriggers accumulated, only five events survive these cuts. Figure 1(a) also shows where an antiproton peak should be on the basis of an extrapolation from the pion and kaon peaks. The five events in Fig. 1(c) are distributed around the extrapolated antiproton peak with a χ^2 of 4.9 for five degrees of freedom. (The probability that a grouping this narrow would arise from a flat distribution over our 50-ns TOF window is less than 10^{-10} .) For these five \bar{p} candidates, information from the intermediate TOF counter is consistent with antiproton TOF rather than that of pions or kaons, and the pulse-height sampling of the CCD system shows clean signals with no indication of pileup.

Figure 2 shows distributions of the summed pulse heights of the eighteen detectors in the lead-glass array. Figure 2(a) shows events identified as pions, and Fig. 2(b) shows the five \bar{p} candidates. Figure 2 shows a broad distribution in equivalent electromagnetic energy, rather than the total energy of the particle. When an incident hadron interacts in the lead glass, some of the resulting particles do not produce Cherenkov radiation proportional to their energy. Thus the mean of each distribution in Fig. 2 lies below the value to be expected if the full available energy were delivered to contained electromagnetic showers (e.g., true π^0 production), although occasionally the full energy of the interaction does get transformed to contained electromagnetic energy. Since the annihilation energy is larger than that for pion interaction, the mean of the \bar{p} distribution is larger than that of the pions. These distributions are consistent with those observed in a similar measurement for \bar{p} and π incident on lead glass.⁷ On the basis of these summed pulse-height distributions, the probability that the five \bar{p} candidates belong to the pion distribution is less than 3% for a modified Wilcoxon rank sum statistic.⁸ The fact that the pulse heights are larger for the \bar{p} distribution than for the pions also discounts the possibility that these events are H^- ions, which should deposit even less ener-

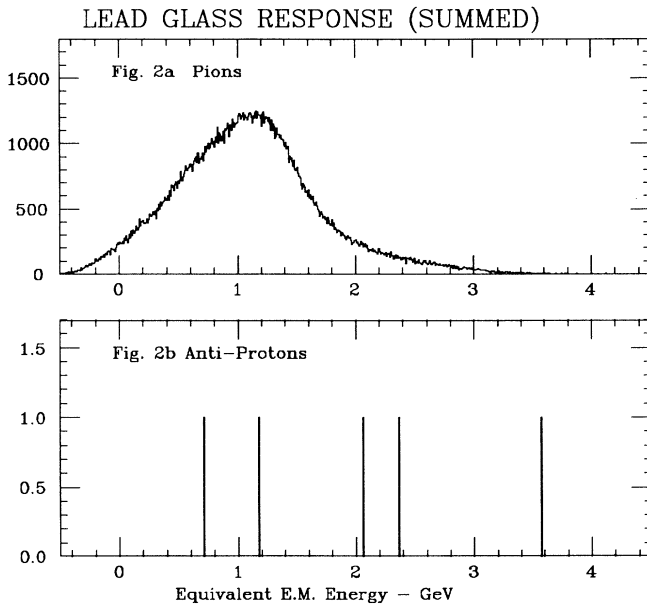


FIG. 2. Lead-glass response (summed) for (a) events identified as pions and (b) the five events identified as antiprotons.

gy than pions. The information from the lead-glass counters thus corroborates our identification of the five events in Fig. 1(c) as antiprotons.

From these results, we obtain a \bar{p}/π^- ratio of 4.3×10^{-7} for secondaries at 1.9 GeV/c and 0° for the reaction $^{28}\text{Si} + ^{28}\text{Si}$ at 2.1 GeV/nucleon. Using pion cross-sectional data from a previous measurement,⁹ we obtain a differential cross section $d^2\sigma/dP d\Omega$ for antiproton production of 80 ± 40 nb/sr (GeV/c).

It is interesting to compare subthreshold antiproton production in nuclear collisions, with that observed in p - A collisions. Figure 3 shows differential cross sections measured for \bar{p} production in p -Cu collisions over a range of incident energies from near the p - p threshold at 6 GeV down to less than 3 GeV.¹⁰ Also shown is the differential cross section for our \bar{p} measurement in Si+Si collisions at 2.1 GeV/nucleon. (In the p -Cu measurements the antiprotons were nearly at rest in the N - N center of mass, while for the Si-Si data the antiprotons had a c.m. kinetic energy of 135 MeV.)

A calculation for subthreshold antiproton production via internal nuclear momentum for p - A and A - A collisions is described in Ref. 11. The calculation employs a double-Gaussian parametrization for the internal nuclear momentum, with parameters for the first Gaussian taken from electron scattering,¹² and the parameters for the second Gaussian taken from data on backward proton production in p - A and A - A collisions.¹³ Only first-chance collisions are considered, with the $N+N \rightarrow \bar{p}+X$ cross section proportional to the available phase space. The calculations were performed at values of the in-

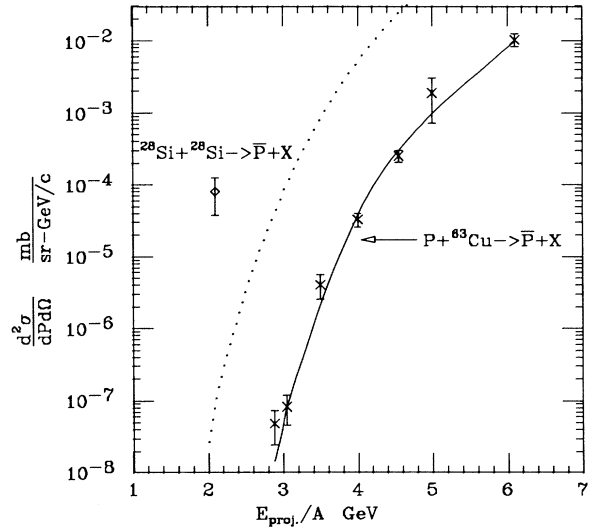


FIG. 3. Subthreshold antiproton production in p +Cu collisions (\times) and a comparison with \bar{p} production in Si+Si collisions (\diamond). Solid line is a calculation for p +Cu $\rightarrow \bar{p}+X$ incorporating a double-Gaussian distribution for the internal nuclear momentum (Ref. 11). Dotted line is the same calculation for Si+Si $\rightarrow \bar{p}+X$.

cident proton energy and outgoing \bar{p} momentum corresponding to the experimental measurement. The solid line in Fig. 3 is a result of fit, where the only variable parameter was the absolute normalization, and the calculated values at the measured points are connected by a smooth line. The excellence of the fit is an indication that down to the levels represented by the data on p +Cu $\rightarrow \bar{p}+X$, no high-momentum components are needed beyond those represented by the double-Gaussian parametrization.

Figure 3 also shows the results of a calculation for \bar{p} production in Si+Si (dashed line) where the internal nuclear momentum is included for both the projectile and target nucleons. A projectile-target mass dependence of $(A_p A_t)^{1.0}$ is assumed. The calculation was made for an outgoing \bar{p} laboratory momentum of 1.9 GeV/c. Our experimental result for antiproton production in Si+Si collisions at 2.1 GeV/nucleon is 3 orders of magnitude larger than expected on the basis of these calculations which satisfactorily account for the effects of internal nuclear momentum in the p +Cu data. Note that these calculations do not fully include the effects of absorption of the \bar{p} in the nuclear medium, which would make the discrepancy even larger.

Subthreshold particle production can occur in a sufficiently equilibrated system. Several models for thermal production of antiprotons have been advanced.^{14,15} Ko and Ge recently suggested¹⁵ that subthreshold \bar{p} production can occur through the reaction $\rho + \rho \rightarrow p + \bar{p}$, where the ρ mesons themselves are produced in the nuclear collision. Their model can predict \bar{p} production at a level

consistent with our observed yield if they assume a thermal mechanism for ρ production, with a ρ abundance given by the equilibrium level at $T=100$ MeV. Recent measurements¹⁶ on electron-pair production in Ca+Ca collisions at 2.1 GeV/nucleon have placed an upper limit on ρ_0 production of 9 mb, which is equivalent to an upper limit on the ρ/π ratio of 6×10^{-3} . However, the equilibrium value for the ρ/π ratio is given by

$$\frac{N_\rho}{N_\pi} = 3 \left(\frac{m_\rho}{m_\pi} \right)^{1.5} e^{-(m_\rho - m_\pi)/T}$$

For a temperature of $T=100$ MeV as assumed by Ko and Ge, the equilibrium ratio for ρ/π is 7×10^{-2} ; over a factor of 10 larger than the experimental upper limit. This casts a serious doubt on the mechanism of $\rho + \rho \rightarrow \bar{p} + p$. Since ρ abundance in nuclear collisions at 2.1 GeV/nucleon appears to be at a level at least an order of magnitude below the equilibrium level, it is doubtful whether thermal mechanisms should be relied upon for subthreshold antiproton production, which would require populating events much further down on the Boltzmann tails than ρ production.

In summary, we have observed subthreshold antiproton production in $^{28}\text{Si} + ^{28}\text{Si}$ collisions at 2.1 GeV/nucleon. The observed \bar{p} yield is about 3 orders of magnitude larger than predicted by a theoretical model which includes the effects of internal nuclear momentum of the colliding nucleons. It has been brought to our attention that subthreshold antiproton production has been recently observed at the Joint Institute for Nuclear Research, Dubna, for C+Cu at 3.65 GeV/nucleon.¹⁷ Although this measurement is at a bombarding energy significantly larger than that reported here, a comparison at different bombarding energies should shed light on the collective mechanism responsible for subthreshold antiproton production in relativistic nuclear collisions.

We would like to thank the engineering and operations

staff of the Bevalac for their support during the experimental program. We would also like to thank P. Braun-Munzinger and G. Young for the loan of the lead-glass counters and access to data on calibration. This work was supported by the Director, Office of Energy Research, Office of High Energy and Nuclear Physics, Nuclear Physics Division of the U.S. Department of Energy under Contracts No. DE-AC03-76S00098, No. DE-FG03-88ER40424, No. DE-FG0288ER40413, and No. DE-FG05-88ER40445.

¹W. Benenson *et al.*, Phys. Rev. Lett. **43**, 683 (1979).

²P. Braun-Munzinger *et al.*, Phys. Rev. Lett. **52**, 255 (1984).

³Y. Le Bornec *et al.*, Phys. Rev. Lett. **47**, 1870 (1981).

⁴J. Miller *et al.*, Phys. Rev. Lett. **58**, 2408 (1987).

⁵J. B. Carroll *et al.*, in *Proceedings of the Eighth High Energy Heavy Ion Study* (LBL Report No. LBL-24580).

⁶S. Carlson *et al.* (to be published).

⁷J. M. Brabant *et al.*, Phys. Rev. **102**, 1622 (1956).

⁸D. B. Owen, *Handbook of Statistical Tables* (Addison-Wesley, Reading, MA, 1962).

⁹E. F. Barasch, thesis, University of California at Davis, 1986 (unpublished).

¹⁰ \bar{p}/π^- ratios from D. E. Dorfan *et al.*, Phys. Rev. Lett. **14**, 995 (1965), and π^- cross sections from A. Shor, V. Perez-Mendez, and K. Ganezer, LBL Report No. LBL-17067 (unpublished); (to be published).

¹¹Shor, Perez-Mendez, and Ganezer, Ref. 10.

¹²E. J. Moniz *et al.*, Phys. Rev. Lett. **26**, 445 (1971).

¹³J. V. Geaga *et al.*, Phys. Rev. Lett. **45**, 1993 (1980).

¹⁴K. A. Olive, Phys. Lett. **95B**, 355 (1980).

¹⁵C. M. Ko and X. Ge, Phys. Lett. **B 205**, 195 (1988).

¹⁶G. Roche *et al.*, Nucl. Phys. **A488**, 477c (1988).

¹⁷A. A. Baldin *et al.*, in *Proceedings of the Third International Conference on Nucleus-Nucleus Scattering, Saint Malo, France, 1988*, edited by C. Detraz *et al.* (North-Holland, Amsterdam, 1988).